Research Article | Vol. 26, No. 16 | 6 Aug 2018 | OPTICS EXPRESS 19964
Optics EXPRESS

Density-dependent determination of scattering properties of pharmaceutical tablets using coherent backscattering spectroscopy

ANNIKA HÄFFNER,* PHILIPP KRAUTER, AND ALWIN KIENLE

Institut für Lasertechnologien in der Medizin und Meßtechnik, Helmholzstr. 12, D-89081 Ulm, Germany
annika.haeffner@uni-ulm.de

Abstract: We report on measurements of coherent backscattering from pharmaceutical tablets. Experimental data is analysed using the radiative transfer equation with focus on the determination of the reduced scattering coefficient μ_s'. The results show a good agreement with μ_s' determined by measuring the spatially resolved reflectance, whereat we demonstrate advantages of the coherent backscattering measurements. Furthermore, we present a correlation between μ_s' and tablet compression force, respectively density.

OCIS codes: (290.7050) Turbid media; (290.5820) Scattering measurements; (290.5825) Scattering theory; (290.1350) Backscattering; (030.1670) Coherent optical effects; (000.4930) Other topics of general interest

References and links

1. M. Blanco, J. Coello, H. Iturriaga, S. Maspoch, and C. De La Pezuela, "Near-infrared spectroscopy in the pharmaceutical industry," Analyst. **123**, 135R–150R (1998).
2. B. Igne, S. Talwar, H. Feng, J. K. Drennen, and C. A. Anderson, "Near-infrared spatially resolved spectroscopy for tablet quality determination," J. Pharm. Sci. **104**(12), 4074–4081 (2015).
3. Z. Shi and C. A. Anderson, "Scattering orthogonalization of near-infrared spectra for analysis of pharmaceutical tablets," Anal. Chem. **81**(4), 1389–1396 (2009).
4. T. Pan, D. Barber, D. Coffin-Beach, Z. Sun, and E. M. Sevick-Muraca, "Measurement of low-dose active pharmaceutical ingredient in a pharmaceutical blend using frequency-domain photon migration," J. Pharm. Sci. **93**(3), 635–645 (2004).
5. C. Abrahamsson, J. Johansson, S. Andersson-Engels, S. Svanberg, and S. Folestad, "Time-resolved nir spectroscopy for quantitative analysis of intact pharmaceutical tablets," Anal. Chem. **77**(4), 1055–1059 (2005).
6. D. Khoptyar, A. A. Subash, S. Johansson, M. Saleem, A. Sparén, J. Johansson, and S. Andersson-Engels, "Broadband photon time-of-flight spectroscopy of pharmaceuticals and highly scattering plastics in the vis and close nir spectral ranges," Opt. Express **21**(18), 20941–20953 (2013).
7. T. Burger, J. Kuhn, R. Caps, and J. Fricke, "Quantitative determination of the scattering and absorption coefficients from diffuse reflectance and transmittance measurements: Application to pharmaceutical powders," Appl. Spectrosc. **51**(3), 309–317 (1997).
8. D. S. Wiersma, M. P. van Albada, and A. Lagendijk, "An accurate technique to record the angular distribution of backscattered light," Rev. Sci. Instrum. **66**(12), 5473–5476 (1995).
9. E. Akkermans, P. E. Wolf, R. Maynard, and G. Maret, "Theoretical study of the coherent backscattering of light by disordered media," J. Phys. France **49**(1), 77–98 (1988).
10. J. D. Rogers, V. Stoyneva, V. Turzhitsky, N. N. Mutyal, P. Pradhan, İ. R. Çapoğlu, V. Backman, "Alternate formulation of enhanced backscattering as phase conjugation and diffraction: derivation and experimental observation," Opt. Express **19**(13), 11922-11931 (2011).
11. P. Krauter, C. Zoller, and A. Kienle, "Double anisotropic coherent backscattering of light," Opt. Lett. **43**(8), 1702-1705 (2018).
12. Y. L. Kim, Y. Liu, R. K. Wali, H. K. Roy, and V. Backman, "Low-coherent backscattering spectroscopy for tissue characterization," Appl. Opt. **44**(3), 366–377 (2005).
13. G. Yoon, D. N. G. Roy, and R. C. Straight, "Coherent backscattering in biological media: measurement and estimation of optical properties," Appl. Opt. **32**(4), 580–585 (1993).
14. A. J. Radosevich, J. D. Rogers, V. Turzhitsky, N. N. Mutyal, J. Yi, H. K. Roy, V. Backman, "Polarized enhanced backscattering spectroscopy for characterization of biological tissues at subdiffusion length scales," J. Biomed. Opt. **17**(11), 115001 (2012).
15. A. J. Radosevich, J. D. Rogers, I. R. Capoglu, N. N. Mutyal, P. Pradhan, V. Backman, "Open source software for electric field Monte Carlo simulation of coherent backscattering in biological media containing birefringence," Phys. Lett. + **18**(4), 1313–1325 (2012).

#328330 https://doi.org/10.1364/OE.26.019964
Journal © 2018 Received 13 Apr 2018; revised 26 Jun 2018; accepted 28 Jun 2018; published 24 Jul 2018

Optics EXPRESS

16. N. Bodenschatz, A. R. Brandes, A. Liemert, and A. Kienle, "Sources of errors in spatial frequency domain imaging of scattering media," J. Biomed. Opt. **19**(7), 071405 (2014).
17. F. Foschum, M. Jäger, and A. Kienle, "Fully automated spatially resolved reflectance spectrometer for the determination of the absorption and scattering in turbid media," Rev. Sci. Instrum. **82**(10), 103104 (2011).
18. V. Busignies, B. Leclerc, P. Porion, P. Evesque, G. Couarraze, P. Tchoreloff, "Quantitative measurements of localized density variations in cylindrical tablets using X-ray microtomography," Eur. J. Pharm. and Biopharm. **64**(1), 38–50 (2006).
19. H. Subramanian, P. Pradhan, Y. L. Kim, Y. Liu, X. Li, and V. Backman, "Modeling low-coherence enhanced backscattering using Monte Carlo simulation," Appl. Opt. **45**(24), 6292–6300 (2006).
20. A. Liemert and A. Kienle, "Spatially modulated light source obliquely incident on a semi-infinite scattering medium," Opt. Lett. **37**(19), 4158–4160 (2012).
21. N. Bodenschatz, P. Krauter, S. Nothelfer, F. Foschum, F. Bergmann, A. Liemert, and A. Kienle, "Detecting structural information of scatterers using spatial frequency domain imaging," J. Biomed. Opt. **20**(11), 116006 (2015).
22. P. Krauter, D. Reitzle, S. Geiger, and A. Kienle, "Determination of three optical properties from subdiffusive spatially resolved reflectance calculations," J. Biomed. Opt. **22**(7), 075003 (2017).
23. P. Krauter, S. Nothelfer, N. Bodenschatz, E. Simon, S. Stocker, F. Foschum, and A. Kienle, "Optical phantoms with adjustable subdiffusive scattering parameters," J. Biomed. Opt. **20**(10), 105008 (2015).
24. F. Foschum, *Bestimmung der optischen Eigenschaften trüber Medien mittels nichtinvasiver Remissionsmessungen*, PhD thesis, Institut für Lasertechnologien in der Medizin und Meßtechnik an der Universität Ulm (2011).
25. Chemical Book, "Cellulose microcrystalline Properties," http://www.chemicalbook.com/ChemicalProductProperty_EN_CB4217927.htm.
26. Chemikal Book, "Sorbitol Properties," http://www.chemicalbook.com/ChemicalProductProperty_EN_CB7183649.htm.
27. L. G. Henyey and J. L. Greenstein, "Diffuse radiation in the galaxy," Astrophys. J. **93**, 70–83 (1941).
28. S. A. Yeboah, S. Wang, and P. R. Griffiths, "Effect of pressure on diffuse reflectance infrared spectra of compressed powders," Appl. Spectrosc. **38**(2), 259–264 (1984).
29. VWR, "Sicherheitsdatenblatt," https://de.vwr.com/assetsvc/asset/de_DE/id/7667884/contents.

1. Introduction

Analyzing backscattered light from optically diffuse scattering media has become a powerful tool in various fields like medical diagnostics, food industry and agriculture. In the pharmaceutical industry, near-infrared spectroscopy is widely used, but demands a complex calibration if used for quantitative purposes [1].

Over the last decades, different methods have been established to separate absorption and scattering, primarily using incoherent light of the visible and near-infrared range. So far, the usage of spatially resolved reflectance [2, 3], frequency-domain measurements [4], time-resolved spectroscopy [5, 6] and measurements of reflectance and transmittance by integrating spheres [7] have been reported in the context of pharmaceutical tablets.

In this study, we demonstrate the successful application of measuring the coherent backscattering (CBS) as a new, calibration-free method for investigating solid pharmaceuticals. The illumination of a sample by spatially coherent light results in an enhancement of the radiance around the backscattering direction, caused by constructive interference [8, 9]. Angularly resolved, the radiance yields a measurable signal closely related to the Fourier transform of the respective spatially resolved reflectance (SRR) signal [10, 11]. While the difficulty of measuring the spatially resolved reflectance increases for strongly scattering media, the CBS cone gets broader which makes it easier to be resolved.

To date, experimental studies on CBS have been reported, investigating other materials than tablets and often using diffusion theory for evaluation [12, 13]. Moreover, subdiffusion scattering in biological media has been investigated [14, 15]. Since it has been shown that using the diffusion equation for determination of the optical properties renders large errors in the spatial frequency domain [16] and thus in CBS (see chapter 3), in this study, the radiative transfer equation (RTE) is used to determine the reduced scattering coefficient μ_s'. In order to validate the results of the CBS measurements, they are compared to results gained by established SRR measurements [11, 17]. Furthermore, a correlation between μ_s' and the tablet density, respectively

Optics EXPRESS

compression force, is found. To date, costly methods like X-ray microtomography are used to measure the density of tablets [18]. Hence, by our findings we initiate the possibility of measuring the density of compressed powders via optical sensors that could be used for process control in the pharmaceutical industry.

2. Experimental setup

A sketch of the used CBS setup is given in Fig. 1. A supercontinuum light source (Fianium

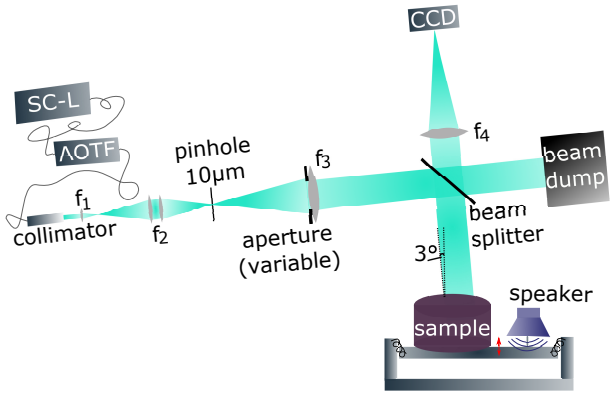

Fig. 1. Schematic representation of the used coherent backscattering setup. SC-L: supercontinuum light source, AOTF: acousto-optical tunable filter, beam splitter: 50/50 plate with AR coating on the left side according to the schematic, $f_1 = 20\,\text{mm}$, $f_2 = 75\,\text{mm}$, $f_3 = 150\,\text{mm}$, $f_4 = 500\,\text{mm}$ (achromatic lenses), beam dump: self-made device consisting of two opposite, black painted mirrors, mounted under angles of 45° respectively −45° relative to the incoming beam direction.

SC450-6) in combination with an acousto optical tunable filter (AOTF, Fianium) is used to generate light around a specific wavelength with full width half maximum of 6 nm. By tuning the AOTF, the center wavelength can be chosen. The setup is optimized for wavelengths in the range of 490 nm to 620 nm. A single mode fiber with an integrated collimator that produces a beam of 3.3 mm diameter is used to transport the AOTF's output ray to a lens system consisting of achromatic components and a 10 μm pinhole. That way, spatial coherence is ensured even for the optional use of other light sources. Afterwards, the beam is collimated by another achromatic lens and divided by a 50:50 beam splitter, where half of the beam vanishes in a beam dump with reflectivity below 0.1 %.

The other part illuminates the sample in an oblique angle of 3°. That way, specular reflections of liquids or plane, polished solids are suppressed. In order to reduce speckle patterns visible for solid samples, they are fixed on a movable platform, which is set under vibration continuously during measurements by a speaker. The distance between the sample surface and f_4 is (32 ± 3) cm, depending on the height of the sample. A Fourier lens images light backscattered from the sample under small angles onto a monochrome CCD chip (QSI 6120s). There, two by two pixels are binned in order to limit the required storage space.

For calibration of the CCD camera, diffraction gratings with 1.62, 2.41 and 3.86 lines/mm have been printed on transparent foil and placed upon the surface of a mirror at the usual sample-position. That way, the diffracted light illuminates several pixel areas of the CCD. Thus, detected distances in units of camera pixels can be assigned to calculated diffraction angles. The setup is able to measure the CBS cone up to 15 mrad with a pixel distance of 12 μrad, related to the binned chip. Moreover, a resolution of <85 μrad is gathered by the full width half maximum of the diffraction spots.

Optics EXPRESS

During the measurement routine, one dark image is taken, followed by 25 sample images that are averaged. By subtracting the dark image from the single sample images, surrounding light as well as reflections from the beam dump and beam splitter are eliminated. This routine is repeated for each wavelength to be measured.

3. Theory and evaluation procedure

Neglecting speckles, the reflectance α of a sample illuminated by spatially coherent light can be described by the sum of an incoherent and a coherent multiple scattering term [9]. As an approximation, these terms are specified using the spatially resolved reflectance $R(\rho)$, where ρ is the distance between the locations of first and last interaction of light with the sample [19]. The angle θ between directions of propagation of incident and reflected light is identified by the change of wave vectors $\Delta\mathbf{k} = 2\pi\theta/\lambda$, yielding

$$\alpha \propto \underbrace{\int_{\mathbb{R}^2} R(\rho) d^2\rho}_{\text{incoherent multiple scattering}} + \underbrace{\int_{\mathbb{R}^2} R(\rho) e^{i\Delta\mathbf{k}\cdot\rho} d^2\rho}_{\text{coherent multiple scattering}} . \tag{1}$$

Perceiving the Fourier transform-like shape of the coherent multiple scattering term, the RTE-solution derived by Liemert and Kienle, originally for the case of a semi-infinite scattering medium and oblique projection of sinusoidal intensity patterns, can be used. In that case, the reflectance is derived depending on the spatial frequency f of the illumination pattern [20, 21]. Accordingly, the absolute value of $\Delta\mathbf{k}$ is identified by the frequency $2\pi f$. The incoherent multiple scattering term corresponds to the reflectance of homogeneous, incoherent illumination and can, according to Eq. (1), be described by the same expression via inserting $f = 0$. In order to limit computational time for evaluating the RTE, its expansion to the seventh spherical harmonic (P_7) is used.

In the experiment, the proportion of the coherent multiple scattering term is weakened due to changes of polarization, among others, that are not included in the described model. Thus, we adapt the equation by adding the enhancement factor η with values between 0 and 1 as already defined elsewhere [8]. Hence, we end up with the description of the angular resolved intensity

$$\alpha \propto SF(f = 0) + \eta \cdot SF(2\pi f), \tag{2}$$

where $SF(f)$ represents the respective RTE solution in spatial frequency domain [20].

In order to match measurement data with this model, values for pixels with the same distance to the backward direction are averaged, yielding the reflectance versus frequency f. As the RTE solution $SF(f)$ depends on the optical properties of the illuminated sample, the reduced scattering coefficient μ_s' and the absorption coefficient μ_a can be be determined by a fit of the averaged measurement data to Eq. (2). These parameters, as well as the enhancement factor η and the constant of proportionality, are adjusted by a trust-region-reflective algorithm.

The evaluation of the SRR data is performed by a fit based on a lookup table of a numerical solution of the RTE. Its start values are determined by a two-dimensional principal component analysis [22], which renders the fit fast and reproducible.

4. Results

We report on our results with focus on the reduced scattering coefficient μ_s', concerning different samples of pharmaceutical tablets. Prior to that, the new CBS method was tested using reliably assessable optical phantoms.

Optics EXPRESS

4.1. Optical phantoms

In order to demonstrate the quality of the new experimental method and evaluation procedure, we present measurement results of three epoxy resin based optical phantoms p1, p2 and p3 that contain different mass concentrations of TiO_2-scatterers (p1: 3.97 ‰, p2: 2.41 ‰, p3: 1.53 ‰). The CBS measurements have been performed using a beam diameter of 15 mm. Details about the manufacturing of the phantoms and former results can be gathered from Krauter et al. [23]. In order to show the accordance of the described theoretical model with the measurement data, Fig. 2 shows the respective curves, exemplarily for the measurements at $\lambda = 562\,\mathrm{nm}$.

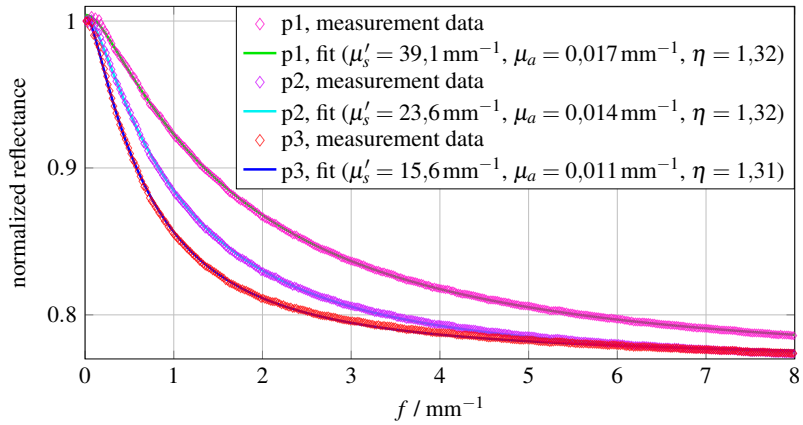

Fig. 2. CBS measurement data and fit results for three epoxy resin based optical phantoms (p1, p2, p3) at $\lambda = 562\,\mathrm{nm}$. The data has been processed as described in section 3 and fitted to Eq. (2), which results in the parameters given in the legend. The enhancement factor of $\eta = 1.3$ can approximately be interpreted as the ratio of the reflectance at $f = 0\,\mathrm{mm}^{-1}$ to the reflectance the curves converge to for large frequencies.

Figure 3 summarizes the results for μ_s' of the phantoms from CBS and SRR measurements.

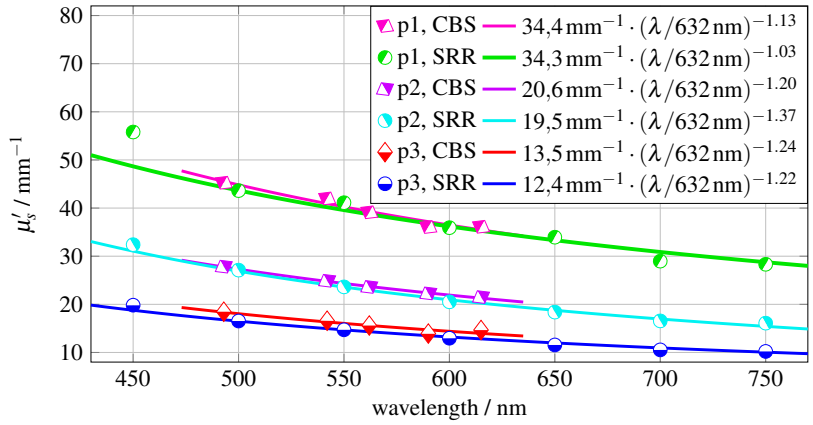

Fig. 3. Reduced scattering coefficients of three epoxy resin based optical phantoms (p1, p2, p3), determined by CBS and SRR measurements. The symbols show the respective measurement data, the lines the results of power law fits.

In both cases, a power law relation of μ_s' versus wavelength fits the data and former results for the phantom system well [24].

Optics EXPRESS

The resulting values of the two different approaches yield relative differences of <10 %, with decreasing differences for increasing reduced scattering coefficients. Moreover, the additional measurement of one of the phantoms in different distances to the detection apparatus showed that the CBS measurements are almost independent of the samples height, observing a standard deviation of only 1.5 % in a range of more than 10 cm height respectively distance difference. SRR measurements, in turn, produce unusable data already for heights deviations of only a few millimeters [17].

4.2. Pharmaceutical tablets of different densities

For the purpose of this study, pharmaceutical powders were compressed to cylindrical tablets of 1 cm diameter under three different forces. Keeping the initial powder volume constant, samples with different mass density and thickness were obtained after compression.

We studied six samples per material and compression force for the two materials avicel and sorbit, using both CBS and SRR measurements. For the CBS measurements, a beam diameter of 0.9 cm has been used in order to illuminate almost the whole sample surface. In Fig. 4, the respective CBS and SRR measurement resemults are shown.

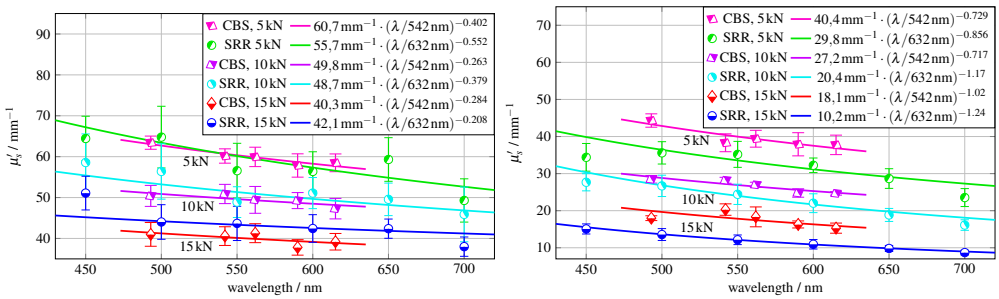

(a) Cylindrical avicel tablets

(b) Cylindrical sorbit tablets

Fig. 4. Reduced scattering coeffitient μ_s' of pharmaceutical tablets compressed by different forces: 5 kN, 10 kN and 15 kN, exercised on a circular area of 1 cm diameter. The symbols represent averages and standard deviations of six samples per kind, determined by SRR and CBS measurements. The lines show the results of power law fits.

Refractive indices of $n = 1.504$ (avicel) [25] and $n = 1.46$ (sorbit) [26] have been adopted. Furthermore, a Henyey-Greenstein type phase function with anisotropy factor of $g = 0.7$ has been assumed for all samples [27]. Again, the widely used power law for μ_s' versus wavelength was fitted, yielding comparable parameters for both methods.

Differences between CBS and SRR data for samples of the same kind could be found, however, they lie within each other's region of tolerance. Concerning the fact that we studied several manually manufactured samples, a natural deviation of their characteristics has to be assumed rather than missing robustness of our methods. Nevertheless, results gained by CBS show noticeably smaller standard deviations. This is presumably due to the almost complete surface illumination and the associated averaging of the light transport over many regions of the sample. Hence, spatial heterogeneity is averaged out, which signifies a distinct advantage of the CBS method, compared to SRR's pencil beam.

Apart from that, the sample height has to be adapted to the different sample thicknesses in every SRR measurement. This source of error is omitted in the CBS measurement, as discussed above. The higher discrepancy of the results concerning sorbit can be attributed to its texture, which has a large influence of the SRR measurements. Rather high variations of resulting mass densities and thereby less homogeneous samples were observed.

Optics EXPRESS

A correlation between compression force and μ_s' can be gathered from Fig. 4 and is further elaborated in Fig. 5. Besides compression force, the resulting mass densities of the tablets have been determined by weighting the single samples using precision scales and measuring the volumina of the cylindrical tablets using a caliper. A relation between optical properties and

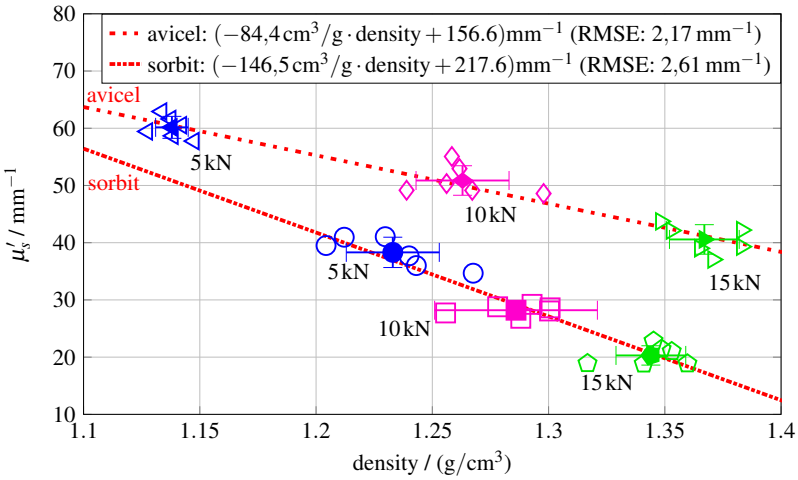

Fig. 5. Correlation between mass density and reduced scattering coeffitient μ_s' at $\lambda = 542$ nm. Linear regression has been performed based on the results for single samples (unfilled symbols). The filled symbols show averages over samples of the same kind.

compacting pressure has previously been reported [28]. However, neither mass density, nor the exact extraction of μ_s' has been taken into account in any previous study, according to our knowledge. Assuming that mainly enclosed air is responsible for scattering, the reduced number or size of scattering centers by decreasing amount of air is a possible explanation for the decrease of μ_s' with increasing mass density.

4.3. *Commercial pharmaceutical tablets*

In addition to measurements on tablet phantoms, we present the applicability of the CBS method to machine-made tablets of commercial purpose. Therefore, acetylsalicylic acid (ASS) tablets of various suppliers and different amounts of active ingredient content were investigated. Thereby, the beam diameter was adjusted to the different sample sizes in order to illuminate preferably a large area (1APharm 100 mg, Ratiopharm 100 mg, Bayer 100 mg: beam diameter of 6 mm; Bayer 500 mg, Ratiopharm 500 mg: beam diameter of 11 mm). The respective results are presented in Fig. 6.

The mass density of ASS exceeds 60 % for all samples. Hence, the refractive index $n = 1.5$ of ASS [29] was adopted. The assumed anisotropy factor is $g = 0.7$. An interrelation between μ_s' and the included component has been observed. Specifically, *Bayer* 500 mg and *1APharm* 100 mg are the only types containing highly-dispersed silicium dioxide and reveal significantly higher values for μ_s'.

Optics EXPRESS

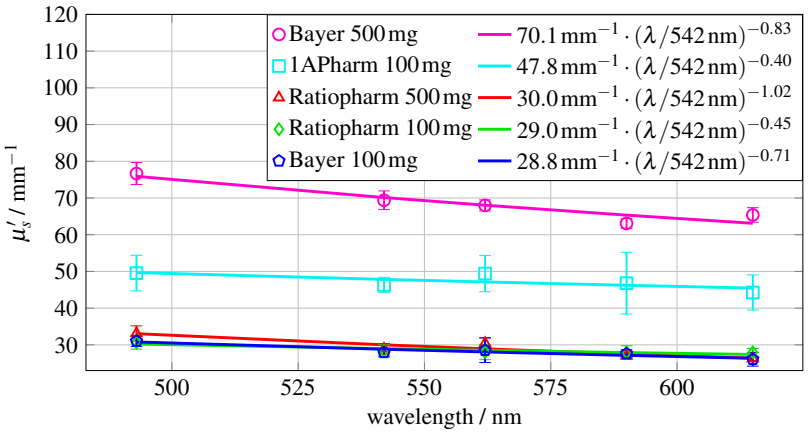

Fig. 6. Reduced scattering coefficients of various ASS tablets, determined via CBS measurement. Mass specifications refer to the amount of active ingredient per tablet, considering that total tablet masses differ from type to type. The symbols represent averaged values of six samples, the lines the results of power law fits.

5. Conclusions

We not only demonstrated the general applicability of the CBS method to pharmaceutical tablets, but also pointed out a correlation between mass density and reduced scattering coefficient. Concerning evaluation, the focus of this study was the reduced scattering coefficient μ_s', determined using the RTE.

Although the used theoretical model fits the measurement data, the neglection of wave characteristics by the RTE has to be kept in mind and shows potential for improvement. Further, the influence of polarization is not quantified yet. A vector RTE solution considering polarization is expected to yield better results than the scalar RTE. Moreover, the range of wavelengths used in this study is rather narrow and will be extended for further studies.

In view of the potential technical application of the CBS method, the fact that it is not sensitive to sample height is advantageous. Furthermore, fluorescence light has no influence on the CBS measurement, in contrast to the compared SRR measurement. Moreover, the resolution of our apparatus in the relevant range of large μ_s' values predestines its application for tablets. The obtained correlation between mass density and μ_s' facilitates the measurement of the former by an optical sensor. The advantages of the CBS method demonstrated above are expected to be applicable for use in industries beyond pharmaceuticals, such as in food industry and agriculture.

Acknowledgments

The authors thank M. Höß and P. Glöggler from ratiopharm GmbH for their support concerning sample preparation and Dr. F. Foschum for his paricipation in that context. P. Krauter acknowledges the support by Evangelisches Studienwerk Villigst e.V.